




Research Article

Theoretical Study on Internal Forces of Primary Support of Tunnel by considering Time Effect

Zhuangzhi Yang ¹, Yuqing Wang, ¹ Lin Song ², and Xinyu Wang ^{3,4}

¹China Railway Tunnel Group Co., Ltd. (Israel), Kfar Saba, Israel

²China Tiesiju Civil Engineering Group Co., Ltd., Heifei, China

³School of Civil Engineering, Henan Polytechnic University, Jiaozuo, China

⁴Key Laboratory of Western Mine Exploitation and Hazard Prevention, Ministry of Education, Xi'an, China

Correspondence should be addressed to Xinyu Wang; wangxinyu2010@163.com

Received 1 February 2020; Accepted 7 April 2020; Published 27 April 2020

Academic Editor: María Criado

Copyright © 2020 Zhuangzhi Yang et al. This is an open access article distributed under the Creative Commons Attribution License, which permits unrestricted use, distribution, and reproduction in any medium, provided the original work is properly cited.

Understanding the internal force distribution and prejudging the weak part of tunnel supporting structure under complicated construction surroundings have become one of the important measures to ensure the safety of tunnel construction. Based on the initial parameter method and field-monitoring results of surrounding rock pressure, the theory of beam on elastic foundation is employed to derive the analytical solution of primary support internal forces. By combining the monitored data of rock pressure in one tunnel, solution of primary support internal force of a section is back analyzed and weak parts of the primary support are analyzed and evaluated. The results show that, after the tunnel excavation is completed, the internal forces of the primary support of the tunnel arch grow larger over time. When $\theta > 1.0$, the internal forces change greatly. The internal force of the primary support decreased to different extents within 2 days after the primary support was applied and then gradually increased over time. Considering the situationality and changeability of the tunnel construction process, the analytical solution for the primary support internal forces of a multicenter arch tunnel proposed in this paper has a strong feasibility in tunnel construction. The conclusions obtained here could provide theoretical support for the design of supporting structure and the optimization of tunnel construction technology.

1. Introduction

One basic concept of the New Austrian Tunnelling Method is to give full play to self-supporting capacity of the surrounding rock, and main safeguard to it is application of the primary support [1–3]. Tunnel excavation is a dynamic construction process. Given the complexity of the geological conditions of tunnel projects and the diversity of tunnel excavation methods, the distribution of internal forces in the concrete supporting structure shows its unique dynamic variation characteristics during tunnel construction. Its actual force state is usually different from that in design condition. Therefore, one of the key measures to ensure safe of the tunnel construction is to investigate distribution of internal forces of the supporting structure and identify the

weak parts of the supporting structure in a timely and accurate manner.

Since the creation of the New Austrian Tunnelling Method, the monitoring and measurement technology has been widely used in tunnel construction. The use of monitoring data to evaluate the safety of tunnel structures and the stability of surrounding rock has become an important means to ensure the safety of the tunnel [4–6].

The back-analysis theory and technology for the tunnel was first introduced to obtain the actual material parameters [7, 8], by using displacements [8–11], stresses [12], or AE monitoring data [13, 14]. In recent years, introduction of new approaches, such as support vector machine [15], particle swarm optimization [16], evolution strategy algorithm [17], and genetic algorithms [18], have promoted the

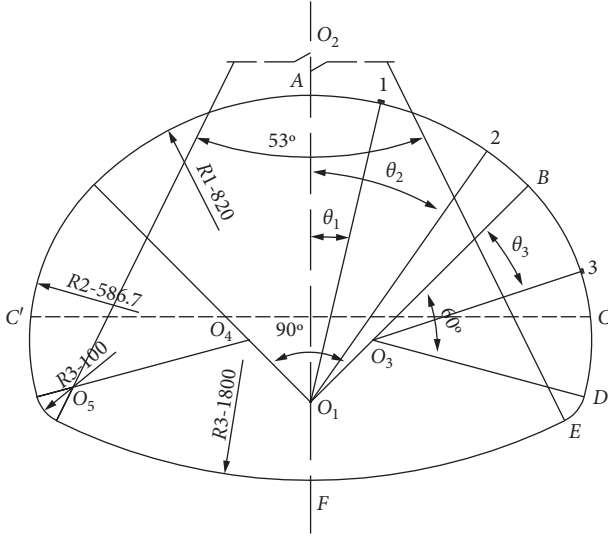


FIGURE 1: Schematic diagram of the tunnel section (unit: cm).

development of back-analysis theory and technology in geotechnical and underground engineering. Moreover, the back-analysis method has been used to investigate the internal forces of tunnel support. Wen et al. [19, 20] proposed analytical solution of internal force of initial support by using the measured touch stresses and steel arch stresses, respectively. On account of theory of the curved beam and straight beam on elastic foundation, Wang and Shao [21] theoretically deduced the inversion formula for internal forces of primary support of the horseshoe-shaped tunnel based on the measured surrounding rock pressure. He et al. [22] presented a novel back-analysis method based on radial displacement and contact stress to evaluate internal forces of the primary support. The initial parameter method [23], since proposed by Vlasov has been used to solve problems of beam column [24] and shell bending [25], while Sun et al. [26] and Wang and Shao [21] obtained internal force of lining and primary support of the tunnel, respectively.

Based on the elastic foundation beam theory and the initial parameter method, the inversion formula to calculate the internal forces of the primary support of the multicenter circular arch tunnel is deduced considering the variation of the measured surrounding rock pressure and the elastic modulus of concrete of the primary support over time. Combined with the measured data of the surrounding rock pressure of the Qixiaying tunnel, the temporal and spatial distribution of the internal forces of the supporting structure is back analyzed. With these efforts, the key parts and time points after the application of the primary support are obtained, and the stability of the primary support is preliminarily determined.

2. Materials and Methods

The section of the Qixiaying tunnel is a multicenter arch section, and the tunnel is excavated with the two-bench method. Figure 1 shows the dimensions of the tunnel section. Figure 2 shows a picture of the upper bench of the Qixiaying tunnel.



FIGURE 2: Picture of the Qixiaying tunnel.

2.1. Control Equation. Primary support of the tunnel excavation can be considered as a curved beam on elastic foundation, and Figure 3(a) shows an arc section of the concrete primary support after excavation of the upper bench. Its inner and outer radii are r_0 and r_1 , respectively. The thickness of the primary support is $h = r_1 - r_0$, the cross-section area is A , and the moment of inertia is I . $r_i = (r_1 + r_0)/2$ is defined as the center radius, and $E(t)$ is the elastic modulus of concrete.

The differential element $r_i d\theta$ is shown in Figure 3(b), where $\omega(\theta, t)$ is the radial displacement, K is the resistance coefficient of the surrounding rock, $M(\theta, t)$ is the bending moment of the cross section, $Q(\theta, t)$ is the shear force, and $N(\theta, t)$ is the axial force. All forces above are considered positive if they point in the direction shown in the figure. If the shear stress between the primary support and the surrounding rock is not taken into account and the second-order trace is omitted, the equilibrium equation of the differential element is as follows:

$$dQ(\theta, t) + N(\theta, t)d\theta + K\omega(\theta, t)r_i d\theta = 0, \quad (1)$$

$$dN(\theta, t) - Q(\theta, t)d\theta = 0, \quad (2)$$

$$dM(\theta, t) - r_i dN(\theta, t) = 0. \quad (3)$$

The radial displacement of the curved beam of the concrete foundation, $\omega(\theta, t)$, is related to the internal forces of the tunnel section as follows:

$$\frac{d^2 \omega(\theta, t)}{d\theta^2} + \omega(\theta, t) = \frac{M(\theta, t)r_i^2}{E(t)I} + \frac{N(\theta, t)r_i}{E(t)A}. \quad (4)$$

By combining equations (1)–(4), the control equation of the radial displacement $\omega(\theta, t)$ can be derived:

$$\frac{d^5 \omega(\theta, t)}{d\theta^5} + 2 \frac{d^3 \omega(\theta, t)}{d\theta^3} + l^2 \frac{d\omega(\theta, t)}{d\theta} = \frac{(M_0 - N_0 r_i) r_i^2}{E(t)I}, \quad (5)$$

where $l^2 = 1 + Kr_1(r_i^3/E(t)I + r_i/E(t)A)$, $M_0 = M(0)$, and $N_0 = N(0)$.

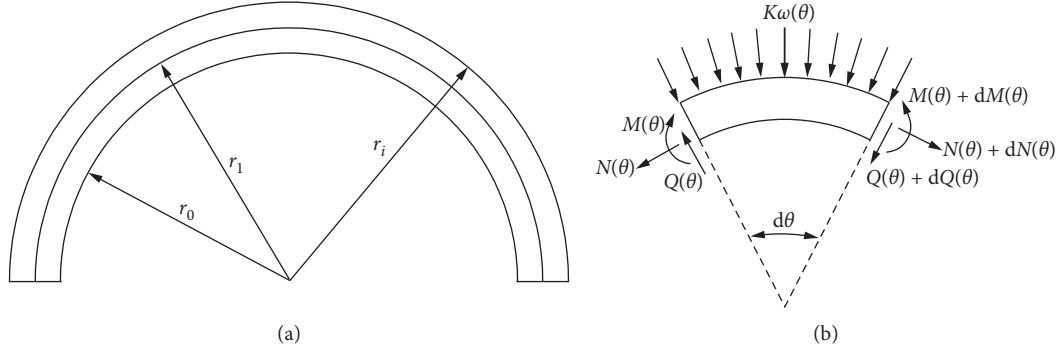


FIGURE 3: Circular beam on elastic foundation [21]. (a) Dimensions of the tunnel supporting structure. (b) Differential element.

2.2. *Internal Forces of Primary Support.* The general solution to the initial parameter of equation (5) is

$$\begin{aligned} \omega(\theta, t) = & e^{-\alpha\theta} (B_1 \cos \beta\theta + B_2 \sin \beta\theta) \\ & + e^{\alpha\theta} (B_3 \cos \beta\theta + B_4 \sin \beta\theta) + \frac{((M_0 - N_0 r_i) r_i^2)}{E(t) I l^2}, \end{aligned} \quad (6)$$

where $\alpha = \sqrt{(l-1)/2}$, $\beta = \sqrt{(l+1)/2}$, and $B_1, B_2, B_3,$ and B_4 are the integral constants.

According to equations (1)–(4) and equation (6), the solutions to the internal forces of the primary support are

$$\begin{aligned} Q(\theta, t) = & \frac{a_M}{r_i} e^{-\alpha\theta} [(\beta B_2 - \alpha B_1) \sin \beta\theta + (\beta B_1 + \alpha B_2) \cos \beta\theta] \\ & - \frac{a_M}{r_i} e^{-\alpha\theta} [(\alpha B_3 + \beta B_4) \sin \beta\theta + (\beta B_3 - \alpha B_4) \cos \beta\theta], \end{aligned} \quad (7)$$

$$\begin{aligned} M(\theta, t) = & a_M e^{-\alpha\theta} (B_1 \sin \beta\theta - B_2 \cos \beta\theta) \\ & - a_M e^{\alpha\theta} (B_3 \sin \beta\theta - B_4 \cos \beta\theta) \\ & + (b_M + 1)(M_0 - N_0 r_i), \end{aligned} \quad (8)$$

$$\begin{aligned} N(\theta, t) = & \frac{a_M}{r_i} e^{-\alpha\theta} (B_1 \sin \beta\theta - B_2 \cos \beta\theta) \\ & - \frac{a_M}{r_i} e^{\alpha\theta} (B_3 \sin \beta\theta - B_4 \cos \beta\theta) + \frac{b_M}{r_i} (M_0 - N_0 r_i). \end{aligned} \quad (9)$$

The angular displacement of the curved beam section $\phi(\theta, t)$ is given by

$$\begin{aligned} \phi(\theta, t) = & \frac{1}{r} e^{-\alpha\theta} [(-\alpha B_1 + \beta B_2) \cos \beta\theta - (\beta B_1 + \alpha B_2) \sin \beta\theta] \\ & + \frac{1}{r} e^{\alpha\theta} [(\alpha B_3 + \beta B_4) \cos \beta\theta + (-\beta B_3 + \alpha B_4) \sin \beta\theta], \end{aligned} \quad (10)$$

where $a_M = \sqrt{l^2 - 1} / ((1/E(t)A) + (r_i^2/E(t)I))$ and $b_M = ((1 - l^2)r_i^2/E(t)I l^2) / ((1/E(t)A) + (r_i^2/E(t)I))$.

TABLE 1: Geometric parameters of primary support.

Arc segment	Inner radius r_0 (cm)	Radius angle θ (rad)
AB	820.0	$\pi/4$
BC	586.7	$\pi/5$
BD	586.7	$\pi/3$

For equations (6)–(10), let $\theta = 0$, and the corresponding initial parameters can be expressed as follows:

$$\begin{cases} \omega_0 = \omega(0), \\ \phi_0 = \phi(0), \\ Q_0 = Q(0), \\ M_0 = M(0), \\ N_0 = N(0). \end{cases} \quad (11)$$

By combining with equation (11), the integral constant ω_0 described by the initial parameter constants $Q_0, M_0, N_0, \phi_0,$ and $B_1 \sim B_4$ is obtained. By substituting the expression of $B_1 \sim B_4$ into equations (6)–(10), the initial parameter formula for the radial displacement of the primary support $\omega(\theta, t)$ with the internal forces $Q(\theta, t), M(\theta, t),$ and $N(\theta, t)$ and angular displacement $\phi(\theta, t)$ is obtained.

The matrix equation between the radial displacement and the internal forces of the primary support expressed by the initial parameter constants is

$$W(\theta, t) = T(\theta, t)W_0 + P(\theta, t), \quad (12)$$

where $W(\theta, t)$ is the radial displacement and internal force array, of which the radius angle with the initial parameter point is θ , W_0 is the radial displacement and internal force array of the known initial parameter point, and $T(\theta, t)$ and $P(\theta, t)$ are the corresponding coefficient matrix and column constant matrix, respectively. $W(\theta, t)$ and W_0 are expressed by $W_\theta = [\omega_\theta, Q_\theta, M_\theta, N_\theta, \phi_\theta]^T$ and $W_0 = [\omega_0, Q_0, M_0, N_0, \phi_0]^T$, respectively.

2.3. *Back Analysis of Internal Forces of Primary Support.* Based on the Winkler hypothesis and the initial parameter method, the analytical formula for the internal forces of the supporting structure of the multicenter arch tunnel described by the surrounding rock pressure is derived.

TABLE 2: Tunnel section parameters.

Parameter	Value
Primary support thickness h (cm)	20
Cross-section area A (cm ²)	2000
Elastic resistance coefficient of surrounding rock K (MPa/m)	480

In Figure 1, the tunnel structure is symmetrical about the center line of the lining. A and F are on the axis of symmetry, and B , C , and D are the intersection points of adjacent arches. Assuming that the tunnel load is symmetrical about the centreline of the tunnel and point A is set to be the starting point of the initial parameter of the primary support, then $Q_A = Q(0) = 0$ and $\phi_0 = \phi(0) = 0$. On that basis, the radial displacement and internal force array of point A is given by

$$W_A = [\omega_A, 0, M_A, N_A, 0]^T. \quad (13)$$

To determine the internal force distribution of arc segments AB and BC of the lining after excavation of the upper bench, we only need to know the three initial parameter constants ω_A , M_A , and N_A of the initial parameter point A in equation (13).

Winkler [27] assumed that the pressure at any point on the foundation is proportional to the deformation of the point, i.e.,

$$P(\theta, t) = K\omega(\theta, t). \quad (14)$$

where $P(\theta, t)$ is the contact pressure between the surrounding rock and the primary support of the tunnel.

According to equations (13) and (14), the solutions for the initial parameter constants ω_A , M_A , and N_A in equation (13) can be obtained from the three measured values of the surrounding rock pressure. The measuring points of the surrounding rock pressure can be arranged at any position in arc segments AB and BC . In Figure 1, the radius angle for the arc between measuring point 1/point 2 and initial parameter point A is θ_1/θ_2 and that for the arc between measuring point 3 and initial parameter point B is θ_3 .

From equation (6)–(10),

$$P(\theta_1, t) = K_{AB}\omega_1, \quad (15)$$

$$P(\theta_2, t) = K_{AB}\omega_2, \quad (16)$$

$$P(\theta_3, t) = K_{BC}\omega_3, \quad (17)$$

where ω_1 , ω_2 , and ω_3 are the radial displacements of the corresponding measuring points of surrounding rock pressure and K_{AB} and K_{BC} are the elastic resistance coefficients of the surrounding rock at the corresponding arc segments.

According to equation (12), ω_1 and ω_2 are in the same arc segment and can be expressed directly by the initial parameter constant of the initial parameter point A . In addition, through the second iteration of point B , ω_3 can also be given by the initial parameter constant of point A .

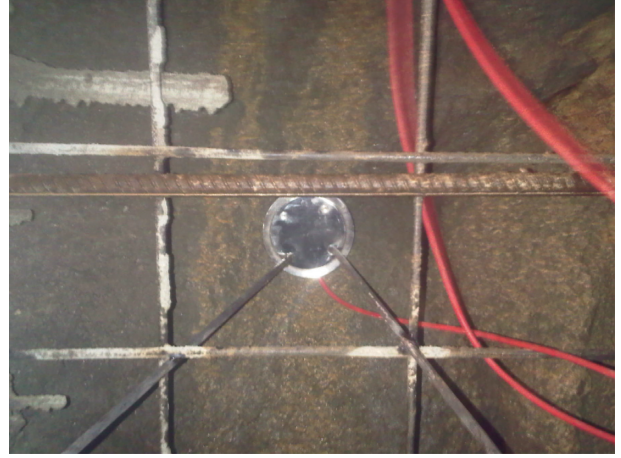


FIGURE 4: Measuring points of surrounding rock pressure.

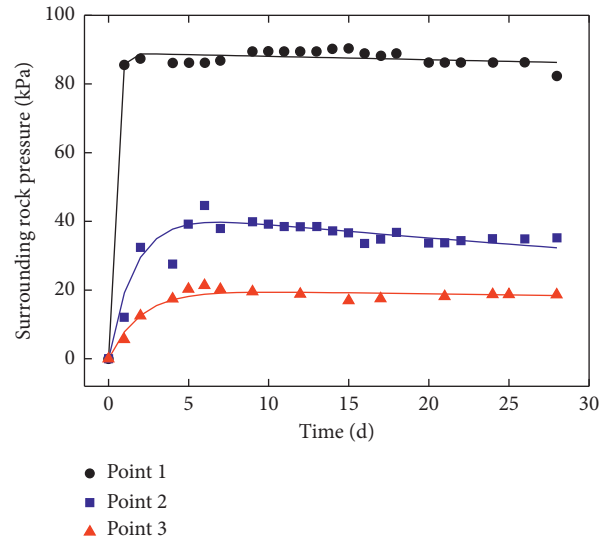


FIGURE 5: Measured rock pressure.

By combining equations (15)–(17), the initial parameter constants ω_A , M_A , and N_A of the initial parameter point A can be calculated. After that, point A is set to be the initial point, and equation (12) is applied segment by segment. In this way, the radial displacement and internal forces of each arc segment of the primary support are found.

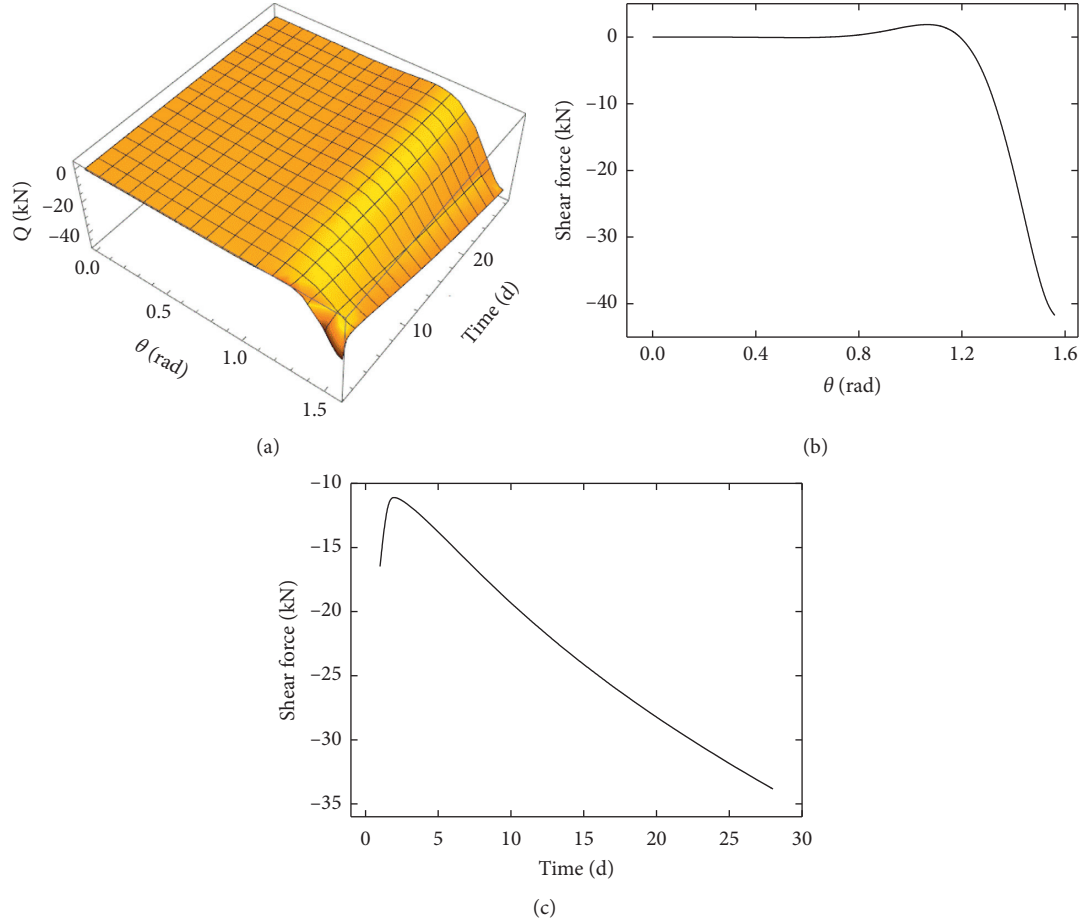
3. Results and Discussion

Based on the results above, the internal forces of the primary support of a multicenter arch tunnel are obtained. For the primary support of the tunnel per unit axial length, the geometric parameters and calculation parameters are shown in Tables 1 and 2.

3.1. Elastic Modulus of Concrete of Primary Support. The left tunnel line K196 + 520 is located at a mileage section, with a strength grade of C20 used in the primary support. The variation trend of the elastic modulus of the concrete with age is defined in the literature as follows [28]:

TABLE 3: Surrounding rock pressure.

Measuring point	Position θ (rad)	Surrounding rock pressure $P(t)$ (kPa)
1	0.09	$89.05 (\exp(-0.001123t) - \exp(-3.328t))$
2	0.61	$43.51 (\exp(-0.01061t) - \exp(-0.6016t))$
3	0.50	$20.15 (\exp(-0.00316t) - \exp(-0.5015t))$

FIGURE 6: Primary support shear force (kN). (a) Temporal-spatial distribution. (b) $t = 28$ d. (c) $\theta = 1.48$.

$$E(t) = 1.05E \left(\frac{(\gamma - \eta)}{(\zeta - \eta)} \right)^{0.8}, \quad (18)$$

where $\gamma = \zeta \exp[-(19.73/t)^{0.6841}]$, $\eta = 0.2819$, $\zeta = 0.8246$, E is the standard value of the elastic modulus of concrete 28 d, and $E = 23$ GPa.

3.2. Surrounding Rock Pressure. At the construction site, TXR-2020 vibrating wire earth pressure cell (as shown in Figure 4) manufactured by Jiangsu Haiyan Engineering Material and Instrument Co., Ltd. was used to measure the surrounding rock pressure of the cross section of the left Qixiaying tunnel line K196 + 520. The measuring points in the section are shown in Figure 1.

Figure 5 shows the measured data for the surrounding rock pressure of the three monitoring points. The solid lines are the results by fitting the measured data. The specific expressions are shown in Table 3.

By substituting the data in Table 3 into equations (15)–(17), the expressions for ω_A , M_A , and N_A are obtained. By combining equations (6)–(9), the distribution of the internal forces of the primary support for the left Qixiaying tunnel line K196 + 520 and the variation trend of the internal forces with time are obtained.

3.3. Analysis of Calculation Results. Figure 6(a) shows the temporal and spatial distribution of the calculated shear force of the primary support. As can be seen from Figure 6(a), for the $\theta \leq 0.74$ arc segment, the shear force of the concrete shows no obvious change with time and space.

Figure 6(b) shows the spatial variation curve of the primary support shear force at $t = 28$ d. From this figure, it can be known that when $\theta \leq 0.74$, the shear force of the concrete shows no obvious change with time and space. When $\theta > 0.74$, the shear force changes greatly with time and space. It converts from positive to negative at $\theta = 1.2$ and

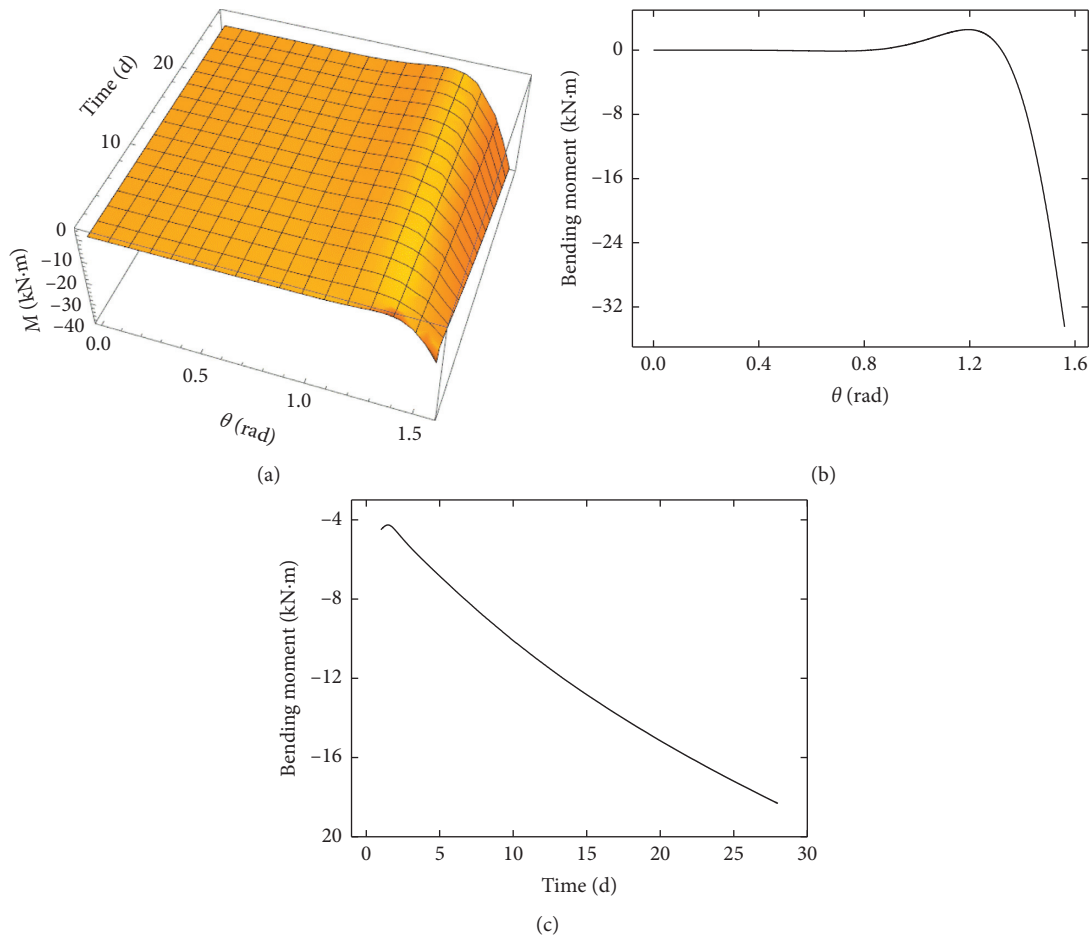


FIGURE 7: Primary support bending moment (kN·m). (a) Temporal-spatial distribution. (b) $t = 28$ d. (c) $\theta = 1.484$.

reaches a maximum value of 41.75 kN at $\theta = \pi/2$. Figure 6(c) shows the variation of the shear force with time when $\theta = 1.484$. It can be seen that the shear force decreases and then increases after the primary support is applied. This trend shall be related to the growth trend of the concrete modulus of the primary support.

Figure 7(a) shows the temporal and spatial distribution of the calculated bending moment of the primary support concrete. As can be seen from Figure 7(a), for the $\theta \leq 0.84$ arc segment, the bending moment of the concrete shows no obvious change with time and space. Figure 7(b) shows the spatial variation curve of the primary support bending moment at $t = 28$ d. It can be seen that at the $\theta \leq 0.84$ arc segment, the bending moment of the concrete shows little change. When $\theta = 1.2$, the bending moment reaches its positive maximum 2.58 kN·m, and when $\theta = \pi/2$, it reaches its negative maximum 35.50 kN·m. Figure 7(c) shows the variation of the bending moment with time when $\theta = 1.484$. It can be seen that the bending moment decreases and then increases after the primary support is applied and reaches the maximum value of 18.32 kN·m at $t = 28$ d.

Figure 8(a) shows the temporal and spatial distribution of the calculated axial force of the primary support. As can be seen from Figure 8(a), for the $\theta \leq 0.98$ arc segment, the axial force of the concrete shows no obvious change with time and

space. Figure 8(b) shows the spatial variation curve of the primary support axial force at $t = 28$ d. It can be seen that when $\theta = 0.88$, the axial force of the concrete is 2.36 kN. With the increase of θ , the axial force reaches its negative maximum 155.37 kN when $\theta = 1.38$ and its positive maximum 214.48 kN when $\theta = \pi/2$. Figure 8(c) shows the variation of the axial force with time when $\theta = 1.31$. It can be seen that the axial force decreases and then increases after the primary support is applied. This trend is consistent with that of the concrete modulus and surrounding rock of the primary support at an early stage.

3.4. Limitation: Unsymmetrical Loading Tunnel. The theoretical inversion model for the internal force of the primary support proposed in this paper applies to the study on the primary support without a closed loop and can estimate the weak part of the primary support. In this model, the surrounding rock pressure on the primary support is bilaterally symmetrical. However, limited by the geological and topographical conditions and route options, the tunnel sections in tunnel entrance, mountain areas, and river valleys are mostly unsymmetrically loaded [29, 30]. Compared with conventional tunnels, the support structure of bias tunnels is more complicated. Therefore, the applicability of the

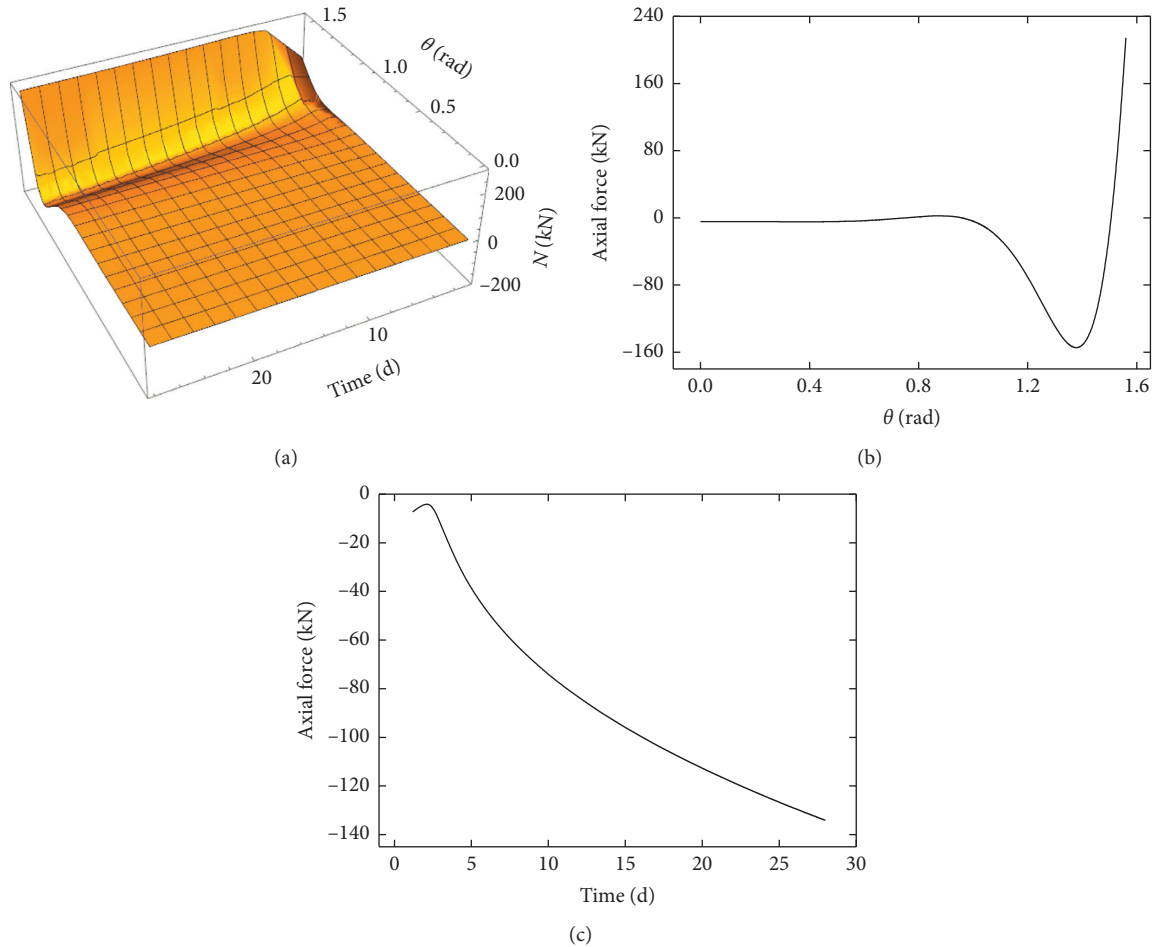


FIGURE 8: Primary support axial force (kN). (a) Temporal-spatial distribution. (b) $t = 28$ d. (c) $\theta = 1.31$.

proposed theoretical model in bias tunnels should be further investigated.

4. Conclusions

Based on the elastic foundation beam theory and the initial parameter method, the inversion formula to calculate the internal forces of the primary support of the multicenter circular arch tunnel is deduced, which takes into account the variation of the surrounding rock pressure and the elastic modulus of concrete of the primary support with time. Combined with the measured data of the surrounding rock pressure of a tunnel, the temporal-spatial distribution of the internal forces of the primary support is back analyzed.

The following conclusions could be drawn:

- (1) After the tunnel excavation is completed, the internal forces of the primary support of the tunnel arch grow larger over time.
- (2) When $\theta > 1.0$, the internal forces change greatly. In particular, the axial force becomes positive when $\theta > 1.5$.
- (3) The internal force of the primary support decreased to different extents within 2 days after the primary

support was applied, and then gradually increased over time.

- (4) The weak part of the primary support of the tunnel constructed with the bench cut method is at the arch foot. On-site observation should be strengthened during construction, and the feet-lock bolt can be applied as necessary.

The analytical expression of the internal force of the primary support concrete proposed in this paper enables fast and real-time determination of the internal force state and stress distribution of the primary support and locates the weak part of the primary support of the tunnel constructed with the bench cut method, so as to provide a basis for safety decision-making in the construction process.

Data Availability

The data generated and analyzed in this study are available from the corresponding author upon reasonable request.

Conflicts of Interest

The authors declare that there are no conflicts of interest regarding the publication of this paper.

Acknowledgments

This research was supported by the Open Fund in Key Laboratory of Western Mine Exploitation and Hazard Prevention of the Ministry of Education under grant no. 2016KF01. The authors gratefully acknowledge this financial support.

References

- [1] I. Ocak, "Control of surface settlements with umbrella arch method in second stage excavations of Istanbul metro," *Tunnelling and Underground Space Technology*, vol. 23, no. 6, pp. 674–681, 2008.
- [2] R. D. Dwivedi, R. K. Goel, M. Singh, M. N. Viladkar, and P. K. Singh, "Prediction of ground behaviour for rock tunnelling," *Rock Mechanics and Rock Engineering*, vol. 52, no. 4, pp. 1165–1177, 2019.
- [3] Y. Yokota, Z. Zhao, J. Shang et al., "Effect of bolt configuration on the interface behaviour between a rock bolt and bond material: a comprehensive DDA investigation," *Computers and Geotechnics*, vol. 105, pp. 116–128, 2019.
- [4] E. Bilotta and G. Russo, "Lining structural monitoring in the new underground service of Naples (Italy)," *Tunnelling and Underground Space Technology*, vol. 51, pp. 152–163, 2016.
- [5] Z. Tang, X. Liu, Q. Xu, C. Li, and P. Qin, "Stability evaluation of deep-buried TBM construction tunnel based on micro-seismic monitoring technology," *Tunnelling and Underground Space Technology*, vol. 81, pp. 512–524, 2018.
- [6] C. Cao, C. Shi, M. Lei, W. Yang, and J. Liu, "Squeezing failure of tunnels: a case study," *Tunnelling and Underground Space Technology*, vol. 77, pp. 188–203, 2018.
- [7] A. Cividini, L. Jurina, and G. Gioda, "Some aspects of "characterization" problems in geomechanics," *International Journal of Rock Mechanics and Mining Sciences & Geomechanics Abstracts*, vol. 18, no. 6, pp. 487–503, 1981.
- [8] Y. Luo, J. Chen, Y. Chen, P. Diao, and X. Qiao, "Longitudinal deformation profile of a tunnel in weak rock mass by using the back analysis method," *Tunnelling and Underground Space Technology*, vol. 71, pp. 478–493, 2018.
- [9] S. Sakurai, S. Akutagawa, K. Takeuchi, M. Shinji, and N. Shimizu, "Back analysis for tunnel engineering as a modern observational method," *Tunnelling and Underground Space Technology*, vol. 18, no. 2-3, pp. 185–196, 2003.
- [10] A. Fakhimi, D. Salehi, and N. Mojtabai, "Numerical back analysis for estimation of soil parameters in the resalat tunnel project," *Tunnelling and Underground Space Technology*, vol. 19, no. 1, pp. 57–67, 2004.
- [11] L. Q. Zhang, Z. Q. Yue, Z. F. Yang, J. X. Qi, and F. C. Liu, "A displacement-based back-analysis method for rock mass modulus and horizontal in situ stress in tunneling—illustrated with a case study," *Tunnelling and Underground Space Technology*, vol. 21, no. 6, pp. 636–649, 2006.
- [12] D. Zou and P. K. Kaiser, "Determination of in situ stresses from excavation-induced stress changes," *Rock Mechanics and Rock Engineering*, vol. 23, no. 3, pp. 167–184, 1990.
- [13] M. Cai, H. Morioka, P. K. Kaiser et al., "Back-analysis of rock mass strength parameters using AE monitoring data," *International Journal of Rock Mechanics and Mining Sciences*, vol. 44, no. 4, pp. 538–549, 2007.
- [14] T.-H. Yang, C. Zheng, P.-H. Zhang, and Q.-L. Yu, "Research on dynamic calibration method of rock mass strength of mine based on microseismic monitoring," *Journal of Mining & Safety Engineering*, vol. 30, no. 4, pp. 548–554, 2013.
- [15] X.-T. Feng, H. Zhao, and S. Li, "A new displacement back analysis to identify mechanical geo-material parameters based on hybrid intelligent methodology," *International Journal for Numerical and Analytical Methods in Geomechanics*, vol. 28, no. 11, pp. 1141–1165, 2004.
- [16] H.-B. Zhao and S. Yin, "Geomechanical parameters identification by particle swarm optimization and support vector machine," *Applied Mathematical Modelling*, vol. 33, no. 10, pp. 3997–4012, 2009.
- [17] N. Moreira, T. Miranda, M. Pinheiro et al., "Back analysis of geomechanical parameters in underground works using an evolution strategy algorithm," *Tunnelling and Underground Space Technology*, vol. 33, pp. 143–158, 2013.
- [18] S. Miro, M. König, D. Hartmann, and T. Schanz, "A probabilistic analysis of subsoil parameters uncertainty impacts on tunnel-induced ground movements with a back-analysis study," *Computers and Geotechnics*, vol. 68, pp. 38–53, 2015.
- [19] J.-Z. Wen, Y.-X. Zhang, and C. Wang, "Back analysis of internal force of initial support in tunnel based on touch stress," *Rock and Soil Mechanics*, vol. 32, no. 8, pp. 2467–2472, 2011.
- [20] J.-Z. Wen, Y.-X. Zhang, C. Wang, and Z.-H. Jiang, "Back analysis for the mechanical properties of initial tunnel support based on steel arch stresses," *China Civil Engineering Journal*, vol. 45, no. 2, pp. 170–175, 2012.
- [21] X.-Y. Wang and Z.-S. Shao, "Theoretical research on the inverse analysis of the internal force of the primary support in a horseshoe tunnel," *Modern Tunnelling Technology*, vol. 51, no. 6, pp. 83–88, 2014.
- [22] W.-Z. He, L.-S. Xu, and L.-L. Wang, "Theoretical back analysis of internal forces of primary support in deep tunnels," *Journal of Engineering Science and Technology Review*, vol. 12, no. 1, pp. 18–26, 2019.
- [23] H. M. Haydl and A. N. Sherbourne, "Elastic buckling of columns by initial parameter method," *Computers & Structures*, vol. 6, no. 2, pp. 127–131, 1976.
- [24] H. M. Haydl, "Bending of cylindrical shells by initial parameter method," *Journal of Engineering for Industry*, vol. 93, no. 3, pp. 845–850, 1971.
- [25] I. V. Orynyak and S. A. Radchenko, "A mixed-approach analysis of deformations in pipe bends. Part 3. Calculation of bend axis displacements by the method of initial parameters," *Strength of Materials*, vol. 36, no. 5, pp. 463–472, 2004.
- [26] F.-X. Sun, X.-H. Cai, and Y.-H. Zhu, "Analytical solution of internal force and displacement in multi-center circular arc tunnel lining based on initial parameter method," *Rock and Soil Mechanics*, vol. 30, no. 4, pp. 1127–1130, 2009.
- [27] L. Zhang, M. Zhao, X. Zou, and H. Zhao, "Deformation analysis of geocell reinforcement using winkler model," *Computers and Geotechnics*, vol. 36, no. 6, pp. 977–983, 2009.
- [28] L. Xu and H. W. Huang, "Time effects in rock-support interaction: a case study in the construction of two road tunnels," *International Journal of Rock Mechanics and Mining Sciences*, vol. 41, pp. 888–893, 2004.
- [29] P.-F. Li, F. Wang, N. Xiong, and C.-P. Zhang, "Methods for calculating rock pressure of symmetrical multi-arch deep tunnels," *Chinese Journal of Geotechnical Engineering*, vol. 38, no. 9, pp. 1625–1629, 2016.
- [30] C. Yang, Z.-X. Hu, D. Huang, and F. Guo, "Failure mechanism of primary support for a shallow and asymmetrically loaded tunnel portal and treatment measures," *Journal of Performance of Constructed Facilities*, vol. 34, no. 1, Article ID 04019105, 2020.